Available online at www.sciencedirect.com
SCIENCE DIRECT®
Applied Surface Science xxx (2006) xxx–xxx
applied surface science
www.elsevier.com/locate/apsusc

Fourier-inversion and wavelet-transform methods applied to X-ray reflectometry and HRXRD profiles from complex thin-layered heterostructures

O. Durand *, N. Morizet

Thales Research and Technology France, Route Départementale 128, F-91767 Palaiseau Cedex, France

Abstract

We show that X-ray scattering techniques can be used for the assessment of individual layer thicknesses inside complicated semi-conductor heterostructures dedicated to the opto-electronic domain. To this end, we propose methods to overcome two main drawbacks coming from: (1) the complexity of the X-ray profiles and, hence the difficulty to use model-dependent tools such as fitting procedures and (2) large dynamics in intensity due to numerous high diffraction superlattice peaks from superlattices which limit the use of the model-independent Fourier-inversion method.

We demonstrate first the reliability of the Fourier-inversion method applied to high-resolution X-ray diffraction profiles curve from quantum well infrared photodetectors heterostructures, complementary to the model-dependent fitting tools. Then, a wavelet-transform-based procedure has been successfully used on X-ray reflectometry profiles containing intense SL Bragg peaks.

Keywords: X-ray reflectometry; High resolution X-ray diffractometry; Semi-conductor heterostructures; Opto-electronic devices; Thickness determination; Fast Fourier transform; Wavelet transform

1. Introduction

Since the 1980s, there has been an increasing interest in the X-ray scattering techniques applied to semiconductor heterostructures dedicated to micro- and opto-electronic devices. Indeed, realization of such devices needs the mastering of the material elaboration in terms of structure, compositions and layer thicknesses. X-ray reflectometry (XRR) allows to determine the depth profile of electronic density, layer thicknesses, defined as distances between mean interfaces, and the one-dimensional RMS interfacial roughnesses, while high resolution X-ray diffraction (HRXRD) is used to infer the depth profile of lattice plane stackings providing the lattice strain state, the number of lattice planes between interfaces and the alloy compositions. For recent years, some innovative approaches for the elaboration of novel semiconductor-based electronic and optical components has induced a high complexity of these heterostructures. Hence, the resulting complexity of both the corresponding X-ray diffraction and X-ray reflectometry profiles has led to the development of both the instrumental and the methodological tools. Among the interpretation data techniques there are either methods based on model-dependent simulation procedures (dynamical theories) [1–3], or methods based on model-independent data-inversion (Born approximation) based on Fourier transform (FT) [4,5]. Let us mention also some model-independent alternative approaches based on semi-dynamical treatment, called distorded born wave approximation, usually applied to the extraction of the electron density profile (EDP) from single thin layers with complicated one-dimensional interfacial roughnesses [6,7].

Concerning the study of both HRXRD and XRR profiles from multilayered materials for micro- and opto-electronics, two main difficulties appear: (1) the increasing complexity of such heterosructures, leading to complex X-ray reflectometry and HRXRD profiles, implies that the direct extraction of information using model-dependent simulation and fitting procedures is becoming very time-consuming, even hazardous

* Corresponding author. Tel.: +33 1 69 41 57 78; fax: +33 1 69 41 57 38.
E-mail address: olivier.durand@thalesgroup.com (O. Durand).

0169-4332/$ – see front matter © 2006 Elsevier B.V. All rights reserved.
doi:10.1016/j.apsusc.2006.05.106

and (2) in most profiles, the presence of numerous high diffraction superlattice (SL) peaks limits the applicability of the model-independent Fourier transform procedure. On previous papers, the use of methods based on the signal-treatment, such as the Fourier-inversion technique to extract the individual layer thicknesses from complex X-ray reflectivity profiles have been reported [5,8]. In this paper, we show the capability of such method for the extraction of the individual layer thicknesses from complex HRXRD profiles. Moreover, most XRR profiles from heterostructures dedicated to opto-electronics display a large dynamic change in intensity due to the presence of numerous super-period peaks. Therefore, applying directly the Fourier-inversion procedure is non trivial. We show here that a wavelet-transform analysis applied to such a complex XRR profile can overcome this difficulty. Using the results from the signal-treatment tools as starting values, fitting procedures can then be used to determine: (1) the EDP through the surface/interface roughness values from XRR profiles and (2) the alloy composition from HRXRD profiles.

2. Experiment

XRR and HRXRD experiments were carried out using a high resolution Seifert PTS goniometer equipped with a two-bounce (XRR) and a four-bounce (HRXRD) Ge(2 2 0) crystal monochromator and a multilayer mirror to enhance the incident intensity.

Two high accuracy incremental encoders allow an absolute angle reading, with an accuracy of 0.0002°, of both the ω and 2θ positions. We have used the Cu $K\alpha_1$ wavelength ($\lambda = 0.1540562$ nm) from a line focus. For reflectometry, the measurements were performed using a detector slit of 0.1 mm. Back Soller slits and a knife edge located at 60 μm from the sample surface allow to decrease the background down to 0.05 cps. Thus, intensity's dynamic range of 10^7 was achieved on the reflectivity curves. For HRXRD, the experiments were performed with a two-bounce Ge(2 2 0)-crystal scattered-beam monochromator, called channel-cut, giving a detector-acceptance-angle of 13 arcsec.

3. Application of signal-treatment on both XRR and HRXRD Profiles

3.1. Fourier-inversion technique

3.1.1. X-ray reflectometry

At small angle of incidence, neglecting the absorption effect, a thin layer is seen as an homogeneous medium with a mean refractive index $n(\lambda) = 1 - \delta(\lambda)$ [9], where λ is the incident wavelength and δ is the order of 10^{-5}, depending on the material. Therefore, the problem of the specular reflectivity of an X-ray beam on a thin layer can be solved using the classical Snell-Descartes and Fresnel relationships applied to thin layers with refraction indices lower than unity. As in the XRD case, the geometry of an XRR experiment is the well-known specular $\theta/2\theta$ one, θ being the grazing angle of incidence and 2θ the angle between the detector and the incident beam. According to the Snell-Descartes expression, a total reflectivity plateau occurs below a critical angle θ_c defined by $\cos\theta_c = n(\lambda)$. In a first approach, XRR can be treated under the kinematical approximation. The reflection coefficient is then proportional to the FT of the electronic density variation along the stack, leading to [4,5,10]:

$$\mathrm{FT}^{-1}_{S_{\mathrm{corr}}}(S^4_{\mathrm{corr}} I(S_{\mathrm{corr}})) = \rho'(z) \otimes \rho'(-z) \tag{1}$$

$\rho'(z)\otimes\rho'(-z)$ is the autocorrelation function (ACF) of the electronic density derivative along z, indicating the interface positions [10,11], and

$$S_{\mathrm{corr}} = \frac{2}{\lambda}\sqrt{\cos^2\theta_c - \cos^2\theta} \tag{2}$$

where S_{corr} is the diffraction vector inside the sample, i.e. corrected from refraction. Hence, the ACF gives the distances between interfaces, i.e. the individual thicknesses and the sum of contiguous thicknesses. In the following, the XRR profiles refers to the $S^4_{\mathrm{corr}} I(S_{\mathrm{corr}})$ curves, i.e. the intensity expressed as I multiplied by S^4_{corr} versus S_{corr}. An estimation of the critical angle value is experimentally inferred taking the angle corresponding to the onset of intensity reduction of the reflectivity plateau. The Fourier-inversion technique applied to XRR profiles is relevant provided that interfaces are well defined, which is generally the case in semi-conductor stackings for opto-electronic devices.

3.1.2. HRXRD

As in a XRR profile, a single-layer thickness can be determined from the thickness fringes (Pendellösung fringes) localized on both sides of a diffraction peak. According to the dynamical theory, the angular gap between the fringes is given by the following relationship [12]:

$$\Delta(\theta_m) = \lambda \frac{\sin\gamma_h}{\sin(2\theta)t} \tag{3}$$

being γ_h is the angle between the diffracted beam and the surface normal, m the fringe order and t is the layer thickness. In the usual case of a specular reflection $\gamma_h = \theta$. Thus, a differentiation of the diffraction vector norm $S = 2\sin\theta/\gamma$, combined with (3) gives:

$$\Delta(S_m) = \frac{1}{t} \tag{4}$$

where S_m is the position of the mth-order fringe, equidistant when positions are expressed in the S-scale. Thus, a FT applied to the single-layer HRXRD profile yields a peak centred on the layer thickness, as in the XRR case. Therefore, we have applied the Fourier-inversion tool on HRXRD profiles to infer information on thicknesses. Some preliminary results on simulated profiles and on an experimental case have already been published elsewhere [5].

However, some care should be taken: (1) definitions of thicknesses are different between both XRR and HRXRD since, in XRR, thicknesses are defined as distances between interfaces, whereas in HRXRD, thicknesses are defined as

coherence lengths of crystalline planes and (2) the kinematical approximation is more restrictive in HRXRD than in XRR since multiple scattering process occurs at diffraction planes instead of at interfaces. Nevertheless, let us mention that: (1) for perfect crystalline thin layers, both thickness definitions are analogous and (2) dynamical phenomenon mainly affects the intensities instead of the angular distances between thickness fringes and super-period peaks [12].

3.2. Wavelet-transform tool

Previous studies have shown the reliability of applying the wavelet analysis on XRR profiles in order to determine both the individual thicknesses and the location of the corresponding layers inside a heterostructure, using the penetration depth variation versus the grazing incidence angle [11]. In our case, we have used the localization property of the wavelets to reduce the dramatic influence of the high intensity SL Bragg diffraction peaks on the ACF spectra. The aim of the wavelet-transform analysis is the same as that the FT analysis, i.e. to decompose the signal $f(S)$ versus a $\psi(S)$ particular base in order to extract the thicknesses values, without the need of any model. The wavelet expression is given by

$$T_f(a,b;\psi) = \int_{-\infty}^{+\infty} f(S)\psi^*_{a,b}(S)\mathrm{d}S \tag{5}$$

$$\psi_{a,b}(S) = \frac{1}{\sqrt{a}}\psi\left(\frac{S-b}{a}\right) \tag{6}$$

being a is the homothetic factor and b is the centring factor. The base $\psi_{a,b}$ chosen for wavelet analysis was the well-known Morlet wavelet (see Fig. 1) [13]. The wavelet extension decays in the S-scale allowing localisation of the signal components. A scalogram $|T_f(a;b;\psi)|^2$ is obtained by the following procedure: the signal $f(S)$ is multiply by the wavelet whose center continuously shifts from small S to higher S. Then the same procedure is applied with a compressed and expanded wavelet (a factor), allowing the decomposition on a higher and a lower frequency, respectively. The scalogram displays some intensity when XRR profile frequency fits the wavelet frequency, giving a frequency analysis in S-scale, which yields the thicknesses and their location in the $(S^4_{\mathrm{corr}}I(S_{\mathrm{corr}}))$ XRR profile.

4. Fourier-inversion technique applied to HRXRD profiles from QWIPs heterostructures

The framework of this study concerns the 8–12 μm infrared (IR) detection [14]. The quantum wells infrared photodetectors

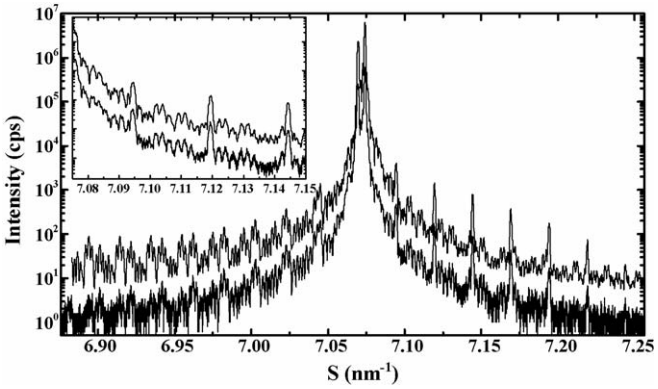

Fig. 2. Experimental (bottom curve) and simulated (upper curve) profiles from a QWIP heterostructure. The simulation has been obtained with the thicknesses values determined using the Fourier-inversion technique described in the text. In inset: zoom on the right side of the substrate peak showing the excellent agreement between both simulated and experimental curves, even for the high frequency fringes.

(QWIPS) heterostructures, grown by molecular beam epitaxy (MBE) on GaAs(0 0 1) substrates, consist of a (GaAs/$Ga_{1-x}Al_xAs$) superlattice (SL) surrounded by thin-layered binary GaAs layers and ternary $Ga_{1-x}Al_xAs$ alloys. The alternating of small-gap GaAs layers and the large-gap $Al_xGa_{1-x}As$ layers defines the artificial quantum wells for the electrons containing two energy states, whose fundamental one is populated with electrons. Under IR illumination, the electrons are excited from the fundamental state into the higher excited one close to the conductive band. Then, these electrons are swept out by an applied electric field, inducing a photocurrent detected by ohmic contacts. It is of crucial importance to determine precisely the thicknesses of all the layers inside the heterostructure. The individual layer thicknesses range over three orders of magnitude, from a few nm to μm. The details of the structure will not be given in this paper. In the following, the FT is applied to the logarithmic scale of the HRXRD profile in order to minimize the intensity's dynamic range. As shown in Fig. 3, a FT applied to a HRXRD profile (Fig. 2) from a QWIP heterostructure displays: (1) peaks related to thicknesses (t1 to t5 in Fig. 3) and sum of contiguous thicknesses and (2) peaks related to the superperiod (SP1 to SP10 in Fig. 3). Taking the positions of some of the SPn peaks, i.e. the 6th, 7th, 8th and 9th orders for example, allows one to infer the value of the superperiod: 40.12 ± 0.05 nm. This value has been confirmed by measuring the slope from the linear regression of n versus S_n, n being the order of the SL-peak at S_n position. The second peak series (t_m) is related to thicknesses and sum of thicknesses from the five thin layers. From their positions the thicknesses of the layers has been inferred. Then, in order to determine the

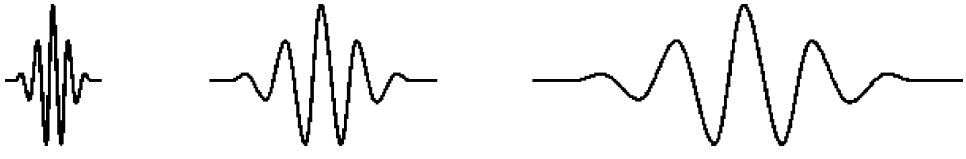

Fig. 1. Morlet wavelet used for the wavelet transform. The wavelet extension decays due to a damping factor. A scalogram is obtained with compression and expansion of the basic wavelet, allowing a decomposition of the signal into frequencies, giving the thicknesses.

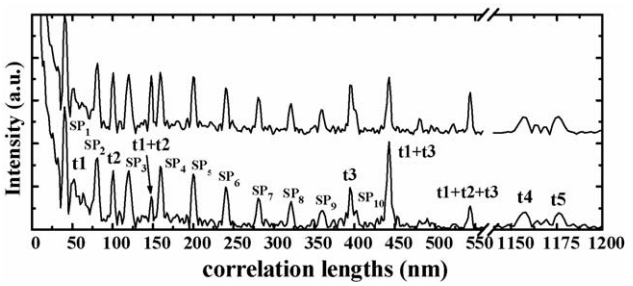

Fig. 3. FT applied to the experimental (bottom curve) and simulated (upper curve) profiles. In the FT applied to the experimental curve, the peaks positions related to thicknesses (from t1 to t5), sum of thicknesses and related to a superperiod (SP1 to SP10) allow a precise determination of all the corresponding thicknesses. The agreement of the peak positions between both FTs confirms the reliability of the Fourier-inversion technique applied to HRXRD profiles.

composition of the $Ga_{1-x}Al_xAs$ alloys from the HRXRD profile, a simulation has been performed using the HR-PTS software, provided by Rich-Seifert & Co., using the thicknesses determined by the Fourier-inversion method as fixed values, i.e. only with varying the *x* and *y* composition values. This software is based on the solution of the Tagaki–Taupin equation (see, for example Ref. [12]) and includes all the dynamic processes. Fig. 2 shows a comparison between both the simulation and the experimental profiles. The fringes are perfectly aligned even in the vicinity of the substrate peak. These fringes are very narrow since they are related to large thicknesses, more than 1 μm. As a confirmation, the FT inversion tool has also been applied to the simulated profile (Fig. 3). The excellent agreement between the FTs from both the experimental and the simulated profiles validates the Fourier-inversion procedure applied to HRXRD profiles. One has to point out the fact that the direct use of a model-dependent simulation procedure is not relevant in the present case. Indeed, to study such a complicated heterostructure, one has to first use a model-independent tool to determine thicknesses values, and then a model-dependent fitting procedure if the alloy compositions are needed.

5. Wavelet-based numerical treatment applied to reflectometry spectra

5.1. Fourier-inversion technique applied to a (GaAs/AlAs)-based waveguide.

(AlAs/GaAs)-based waveguides were designed for frequency generators [15], using the large nonlinear susceptibility of GaAs for parametric conversion. The nominal wave-guide structure was: $4 \times$ [GaAs(383 nm)/AlAs (37.5 nm)]/$Al_{0.70}Ga_{0.30}As$ (digital alloy, 1000 nm thick)//GaAs(0 0 1) grown by MBE. The digital alloy is a $530 \times$ (GaAs 0.85 nm/AlAs 1.98 nm) superlattice. The result of the thicknesses determination by the Fourier-inversion technique applied to the XRR profile has already been published elsewhere [5]. Due to the presence of huge Bragg diffraction peaks (from the digital alloy), the Fourier transform has not been applied directly to the XRR profile. Indeed, we have completely eliminated the intensity's dynamic range by reconstructing the XRR spectra by a ''triangle function'' in which minima (zero intensity) and maxima (intensity equal to one) are related to the minima and maxima of the experimental spectra (Fig. 4). The FT transform has then been applied to the reconstructed profile, yielding 35.09 ± 0.05 nm for the AlAs layers and 385.5 ± 0.5 nm for the GaAs layers.

5.2. Wavelet-transform numerical treatment applied to a (GaAs/AlAs)-based waveguide.

As shown previously, the presence of high intensity diffraction peaks is a considerable drawback for the applicability of the Fourier-inversion technique. Therefore, we have applied the wavelet transform to the XRR profile from the

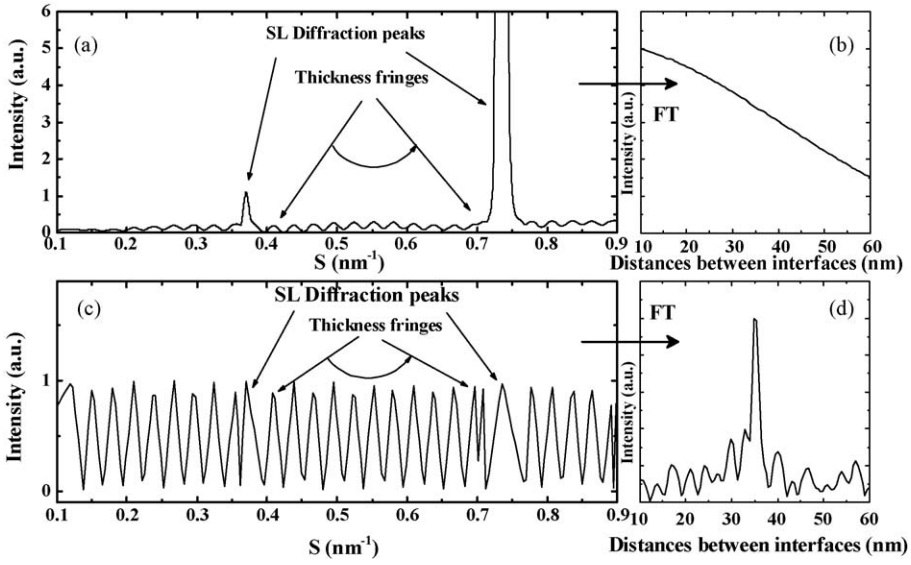

Fig. 4. (a) Example of a XRR profile displaying two SL Bragg peaks and (b) corresponding FT. (c) Reconstruction of the XRR profile, in (a), by a ''triangular function'' (see text) and (d) corresponding FT showing a peak related to the thickness fringes.

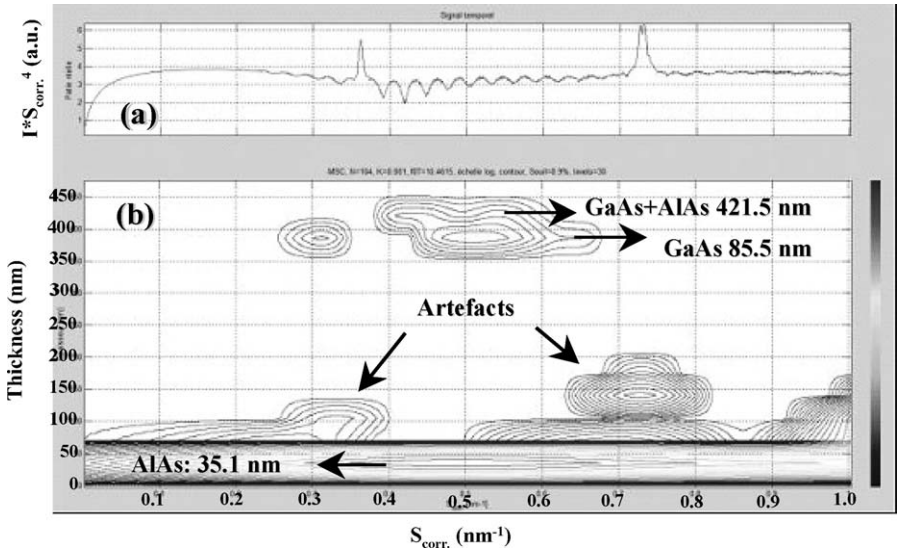

Fig. 5. (a) XRR from the waveguide heterostructure, drawn in log scale. (b) Scalogram, i.e. thicknesses vs. S_{corr} representation, obtained by applying wavelet transform to the XRR profile.

(GaAs/AlAs)-based waveguide. The corresponding scalogram, shown in Fig. 5, consists in a thickness versus S_{corr} representation. Two streaks, parallel to the S-scale, correspond to the thicknesses from the AlAs layers (35.1 nm) and from the GaAs layers (385.5 nm). The third streak (421.5 nm) is related to the sum of these two thicknesses. These values are consistent with the results obtained by the Fourier-inversion technique applied to the triangle-function reconstructed-profile. The extension in S-scale of these streaks corresponds to the location of the corresponding thickness fringes in the XRR profile. One can notice the artefacts from the SL Bragg peaks which yield figures at the corresponding S_{corr} positions. These artefacts do not affect the results of the thickness determination since they are localized in S_{corr}, which is due to the localization of the wavelet. Therefore, this example shows the reliability of using the wavelet transform to study XRR profiles which contains SL Bragg diffraction peaks.

6. Conclusion

The reliability of using both the Fourier-inversion and the wavelet-transform methods to study fine-structured HRXRD and XRR profiles from complicated heterostructures has been demonstrated. Solutions have been proposed to overcome two main drawbacks related to the difficulty of applying directly the well-known model-dependent fitting procedures and other to the presence of high-intensive SL Bragg peaks which limits the use of the Fourier-inversion method. A QWIP heterostructure has been successfully studied by HRXRD using first the Fourier-inversion technique, usually dedicated to XRR, to assess all the individual layer thicknesses and then using a fitting procedure to determine only the alloys composition, using the results of the Fourier-inversion method as input (and fixed) parameter. An XRR profile from a wave-guide heterostructure, displaying SL Bragg peaks, has been studied by wavelet transform. We have shown that the localized nature of the wavelet overcomes the problem due to the presence of the SL Bragg peaks and allows an accurate thickness determination with a determination of the corresponding fringes localisation in the XRR profile.

Acknowledgements

The author would like to acknowledge X. Marcadet for providing excellent-quality MBE-grown samples and E. Smigiel for helpful discussions.

References

[1] P.F. Fewster, 2nd ed., X-ray Scattering from Semiconductors, vol. 44, Imperial College Press, London, 2003, pp. 31–103.
[2] A. Ulynenkov, Proc. SPIE 5536, 2004, p. 1.
[3] L. David, I.M.D. Windt, Software for modelling the optical properties of multilayer films, Comput. Phys. (1998).
[4] F. Bridou, B. Pardo, J. X-ray Sci. Technol. 4 (1994) 200–216.
[5] O. Durand, Thin Solid Films 450 (2004) 51–59.
[6] S. Banerjee, S. Chakraborty, P.T. Lai, Appl. Phys. Lett. 80 (2002) 3075.
[7] A. van der Lee, J. Phys. IV (France) 12 (2002) Pr6–Pr255.
[8] O. Durand, A. De Rossi, A. Bouchier, J. Phys. IV (France) 118 (2004) 203–211.
[9] B. Vidal, P. Vincent, Appl. Opt. 23 (1984) 1794.
[10] F. Bridou et, B. Pardo, J. Phys. III (France) 4 (1994) 1523.
[11] E. Smigiel, A. Cornet, J. Phys. D: Appl. Phys. 33 (2000) 1757–1763.
[12] High-resolution X-ray scattering from thin films and multilayers, V. Holý, U. Pietsch, T. Baumbach (Eds.), Tracts in Modern Physics, vol. 149, Springer, Berlin, Heidelberg, 1998.
[13] C. Chui, in: C. Chui (Ed.), An Introduction to Wavelets, Academic Press, New York, 1992.
[14] E. Costard, P. Bois, X. Marcadet, F. Audier, E. Herniou, in: Proceedings of the SPIE/Infrared Technology and Application XXV, Orlando, 1999, p. 3436 (MWIR Quantum Well Infrared Photodetectors).
[15] A. Fiore, V. Berger, E. Rosencher, P. Bravetti, J. Nagle, Lett. Nat. 391 (1998) 463.